ELSEVIER

Surface Science 440 (1999) 231–251

surface science

www.elsevier.nl/locate/susc

The interaction of copper with a rhenium(0001) surface: structure, energetics, and growth modes

R. Wagner, D. Schlatterbeck [1], K. Christmann *

Institut für Physikalische und Theoretische Chemie der Freien Universität, Takustr. 3, D-14195 Berlin, Germany

Received 17 May 1999; accepted for publication 7 July 1999

Abstract

Thin Cu films were vacuum-deposited onto Re(0001) and investigated by means of temperature-programmed desorption spectroscopy (TDS), X-ray photoelectron spectroscopy (XPS), low-energy electron diffraction (LEED), and Auger electron spectroscopy (AES). TDS (performed with a heating rate of 7.7 K/s) reveals three (coverage-dependent) Cu binding states β_3, β_2, and β_1 between 1000 and 1200 K associated with Cu monolayer and multilayer formation, respectively. While the second and multilayer states β_2 and β_1 exhibit clear zero-order kinetics, the first monolayer state desorbs with more complicated desorption kinetics due to attractive mutual Cu–Cu interactions. The activation energy for desorption varies between $\sim$200 kJ/mol for vanishing Cu coverage and $\sim$320 kJ/mol near the monolayer saturation. Cu grows first pseudomorphically and forms, between 2 and 3 ML, an incomplete (14×14) LEED structure (only first- and second-order diffraction spots are visible). At larger coverages, the formation of genuine Cu(111) crystallites is indicated by a Cu(1×1) LEED pattern. AES and XPS suggest an incomplete Stranski–Krastanov growth mode, since the Re signals remain visible even after deposition of 12 nominal Cu layers. The absence of any Cu and Re core level shifts in XPS (to within the resolution of our instrument) points to a negligible chemical interaction between the two elements at the interface.

Keywords: Copper; Growth; Rhenium; Surface energy; Surface structure and morphology; Thermal desorption spectroscopy

1. Introduction

The still increasing number of publications concerned with thin metallic films clearly underlines the scientific and practical importance of these materials [1–4]. Especially applications in optical coating technology, composite materials and in the field of heterogeneous catalysis must be mentioned here. For catalytic purposes, morphology and structural stability of the thin film are of vital interest, while surface physicists often examine elementary processes of nucleation and growth including an analysis of the underlying kinetic and energetic reaction steps.

According to our current understanding of heteroepitaxy [5–7], these processes are believed to primarily depend on (i) the 'chemical' affinity between the deposit and the host material, and (ii) how well their geometrical lattice parameters match. In order to obtain more information about this latter influence, we started a series of systematic investigations in which we chose a given host surface and varied the (chemically similar) deposited material with respect to its lattice parameters.

* Corresponding author. Fax: +49-30-838-4792.
E-mail address: kchr@chemie.fu-berlin.de (K. Christmann)
[1] Present address: Schott-Glaswerke, Postfach 2480, D-55014 Mainz, Germany.

0039-6028/99/$ – see front matter
PII: S0039-6028(99)00805-5

As pointed out previously, we have selected the rhenium(0001) single crystal face as this 'standard' host surface, because it provides a very smooth (but comparatively rigid) hexagonal lattice (mean corrugation amplitude ≤ 0.1 Å). Furthermore, it is thermally stable up to more than 3000 K and can be cleaned effectively by a combined oxidation/reduction procedure as described elsewhere [8]. Accordingly, deposited noble metals that do not form bulk alloys with Re can be effectively removed by simple thermal desorption.

In continuation of previous work with silver films [9,10], we have studied the nucleation and growth as well as the energetics and kinetics of the desorption reaction of copper thin films deposited on the Re(0001) surface; a respective work using gold thin films is in progress. With its filled 3d band Cu is chemically relatively inert; it behaves like an electron-rich sp-metal and has, according to its position in the periodic table, close similarities to Ag and Au. Its surface free energy is tabulated as 1.825 J/m^2 [11]. Rhenium, on the other hand, is a refractory metal and exhibits, due to its extremely high cohesive energy, also a very high surface free energy (3.60 J/m^2), roughly twice the Cu value [11]. For a very recent useful compilation of (theoretical and experimental) surface free energies, we refer to an article by Vitos et al. [12]. Interestingly, both metals possess identical Pauling electronegativities [13], resulting in an almost vanishing mutual chemical reactivity, i.e. a polarization of a Cu–Re bond does not take place. As another consequence, Cu and Re are immiscible in the bulk [14,15] and crystallize in different lattices: Cu is face-centered cubic (fcc), with a nearest-neighbor distance of 2.5509 Å, and Re is hexagonal close-packed (hcp), with a nearest-neighbor distance of 2.7609 Å. Hence, a Cu atom is by $\sim 8.2\%$ smaller than a Re atom, and the resulting negative lattice misfit is likely to affect the Cu growth behavior.

The Cu/Re(0001) system has been studied before, especially in the laboratory of D.W. Goodman [16–19]. Among others, its structural and energetic properties were explored by means of low-energy electron diffraction (LEED), thermal desorption spectroscopy (TDS), Auger electron and electron energy loss spectroscopy (ELS) [16], as well as by X-ray photoelectron spectroscopy (XPS) [17]. The authors report on the appearance of various LEED patterns, two TD states β_1 and β_2 and a comparatively small chemical interaction between Cu and Re as indicated by the practically unaffected XPS Cu $2p_{3/2}$ core level binding energy in Cu films deposited on Re. A total shift in the electron binding energy of ~ 0.15 eV was reported between submonolayer Cu coverages and a 20 ML Cu film [19]. In a subsequent article, He and Goodman also studied the adsorptive and catalytic properties of the Cu-on-Re(0001) system with respect to hydrogen, carbon monoxide, and nitrogen [17]. In our work here, we will conduct a detailed comparison between Goodman's results and our data and will demonstrate that at least some of the previous conclusions need to be modified.

For a better understanding of the physical properties of the interaction system, a comparison with the ruthenium(0001) surface covered with Cu deposits can also be helpful. Ru(0001) exhibits some similarities with Re(0001), even in catalytic respects, and numerous investigations were performed with Cu films condensed on Ru(0001) [20–25]: scanning tunneling microscopy (STM) investigations revealed a peculiar pyramidal, quasi-3D structure of the Cu films in which at least 10 subsequent monolayers are populated simultaneously [22,23].

In the following, we will particularly focus on the energetic and kinetic behavior (as probed by a precise computer-controlled data evaluation of TD spectra, see below) and on the growth morphology (as monitored by LEED, AES, and XPS). We will demonstrate that our data and analysis go beyond the previous report by He and Goodman [16], especially as far as the observation of LEED structures and the features of the TD spectra are concerned. A detailed comparison of our data with the previously investigated Ag/Re(0001) system [10] will provide an insight into how geometrical lattice misfit influences the growth behavior of a two-dimensional metallic film. In a forthcoming article, we will present information on the morphology of the Cu/Re(0001) system deduced from STM [26].

2. Experimental

The measurements were carried out in an ultra-high vacuum (UHV) system equipped with the standard facilities to clean and characterize a metal single crystal surface, among others LEED, AES, XPS, and TDS. Since the apparatus has been described in detail previously [9], we can keep this section short. A combined ion getter and turbomolecular pumping system, along with a Ti sublimation pump, routinely provided pressures in the 10^{-11} mbar range; even during prolonged Cu deposition (see below), the pressure did not rise beyond 5×10^{-10} mbar.

The sample consisted of a cylindrical Re single crystal of 5 N purity (10 mm diameter, 1 mm thickness) which was X-ray oriented to within 0.5°. The crystal was spot-welded to two parallel-running tantalum wires; a 5% ReW/25% ReW thermocouple was attached to the side of the sample. Initial cleaning was achieved according to the following routine: (i) short heating to 2300 K; (ii) 2 min heating at 1800 K in an oxygen atmosphere ($p_{O_2}=3\times10^{-8}$ mbar); (iii) short flash to 2300 K; (iv) 10 min heating at 1120 K in a hydrogen atmosphere ($p_{H_2}=2\times10^{-7}$ mbar); and (v) 10 s flash to 2300 K. After this treatment the Re sample showed the typical hexagonal (1×1) LEED pattern with sharp and bright spots on a negligible background; neither in AES nor in XPS were any C, O, or S impurities detectable.

Copper deposition was accomplished by subliming electrolyte Cu (4 N purity) from a commercial Knudsen oven (WA Technology) operated at the (electronically controlled) temperature of 1300 ± 1 K. In most of our experiments, a standard deposition rate of ~1 ML/min was chosen. The surface temperature was adjusted to 673 K, only during the XPS and AES measurements $T=625$ K was chosen. In some cases we annealed the deposits up to temperatures of 973 K. Calibration of the Cu monolayer coverage is based on combined TDS and XPS measurements as pointed out further below.

Our Cu source provided a very linear deposition rate as judged from the linearity of a plot of the Cu coverage (taken from the integrated area of Cu TD spectra, $\int p_{Cu}\,dt$) versus evaporation time, for a deposition temperature of 673 K. The resulting curve does not exhibit any systematic change in slope, even after deposition of more than six Cu monolayers. (The deposition rate in this case was 1.1 ML/min.) Therefore, we deduce a constant (and high) Cu condensation coefficient spanning the monolayer and multilayer regime.

As will be shown in Section 3, TDS is one of the main sources of information. In this and previous work [10], we have improved the TDS experiment by (i) precisely controlling the sample positioning with respect to the mass spectrometer, (ii) keeping track of the linearity of the sample heating, and (iii) using a sophisticated computer-controlled data acquisition and evaluation procedure. Since a more elaborate description will be given in a forthcoming work [27], we present only some useful details here. In our TDS experiments, mostly two different TDS heating ramps were used, namely 7.7 and 21.7 K/s. The heating itself was accomplished by electron bombardment (sample on high voltage potential), the anode voltage being controlled by a PID device and a personal computer. It turned out that the reproducibility of the TDS traces depends crucially on the sample position with respect to the mass spectrometer. Therefore, in order to provide a constant aperture angle for collecting the desorbing Cu atoms, we moved a plate with a small circular hole (3 mm diameter) between the sample and the ionization source of the quadrupole mass filter and mounted a high-precision linear motion drive to our sample manipulator [28].

Concerning the TDS data handling, we first subtracted the background (caused by a spurious hydrocarbon mass) by a linear interpolation between the starting and ending point on the temperature axis. No further smoothing was employed at this stage. All spectra were calibrated with respect to the spectrum of the first Cu monolayer ($\Theta=1.0$ ML). The procedure was as follows. From a so-called layer plot [29] (later shown as Fig. 2), in which we plotted the Cu desorption rate against the relative Cu coverage (TDS peak integral), we inferred the exact monolayer coverage as the largest Θ value that does not yet contain contributions from the second Cu monolayer. Clearly, the layer plot provides this information

more accurately than the 'normal' set of TDS spectra.

The second important source of information is X-ray photoelectron and Auger electron spectroscopy, and we add also a brief description of the XPS (AES) experiment. We used Al Kα radiation (1.4866 keV) and a 2.4 keV primary electron beam, respectively. The secondary electrons emitted from the sample were collected by means of a spherical electron energy analyzer (CLAM II, resolution ~200 meV); the XP spectra were taken using a constant analyzer voltage of 50 eV, the AE spectra using a constant retard ratio of 0.25.

3. Results

In this section, we will present our data in the sequence TDS, LEED, XPS, and AES, with particular emphasis on the TDS results.

3.1. Temperature-programmed desorption spectroscopy

TDS is a very powerful tool to probe the physical and chemical properties of adsorbed layers as repeatedly pointed out previously [30–34]. From a careful analysis of a series of TDS spectra, information on the energetics and kinetics, and hence on the mechanism of the desorption reaction as well as on the adsorbate coverage prior to the application of the temperature program, is available. From this, conclusions about the growth mode of the deposit material can be drawn. In the following we will emphasize the issues of *coverage determination* and *growth mode* and thereafter focus on the analysis of the desorption *kinetics* and *energetics*.

A representative set of Cu thermal desorption spectra is shown in Fig. 1. The spectra were taken with a heating rate $\beta = dT/dt$ of 7.7 K/s up to an

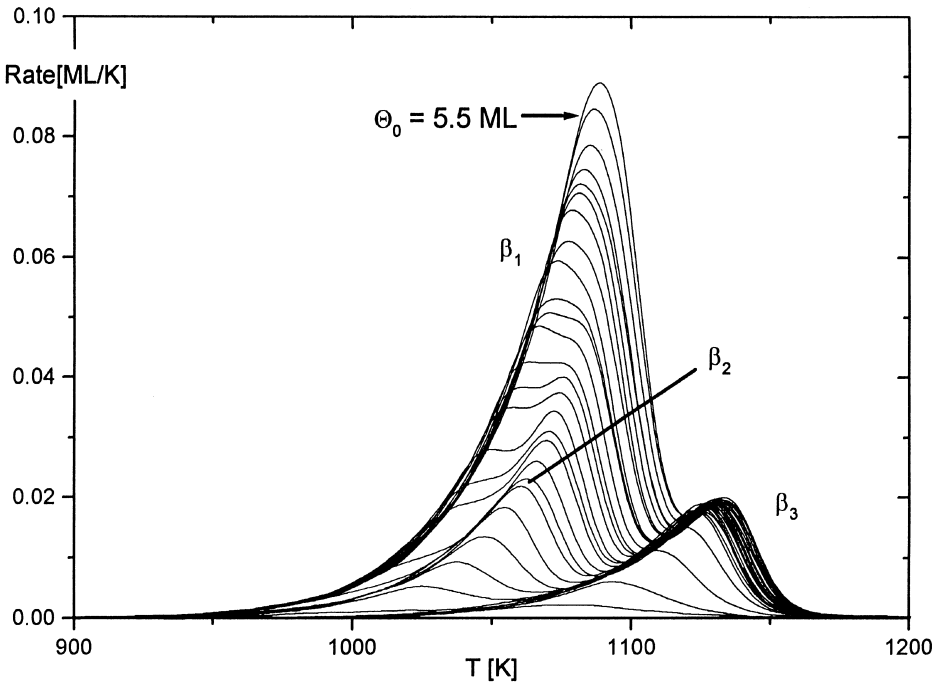

Fig. 1. Series of Cu thermal desorption spectra obtained from a Re(0001) surface with a heating rate of 7.7 K/s. The Cu deposition was performed at 673 K up to a coverage of 5.5 ML. The parameter of the curves is the initial coverage. Clearly, the first and second monolayer states (β_3 and β_2) and the third + multilayer states (β_1) can be distinguished.

initial coverage of 5.5 ML equivalents. Three desorption states β_1, β_2, and β_3 can be clearly distinguished. Under our experimental conditions the (highest-lying) β_3 state (reflecting the first Cu monolayer) appears at 1120 K (maximum position at saturation), while the saturated β_2 state (associated with the second monolayer) has its maximum desorption rate at 1055 K. As the Cu deposition is continued, the β_1 state grows in (at $\Theta = 3$ ML, its maximum appears at 1035 K) and finally dominates the entire TD spectrum. After a coverage of $\sim$20 ML, the two other states, β_3 and β_2, are practically obscured by the overall β_1 desorption. We tried to resolve another TDS state within the coverage interval in which the third layer becomes covered by the fourth Cu layer. Therefore, we reduced the heating rate β to merely 2.1 K/s. Despite the higher resolution, no fourth state could be delineated, instead all TDS maxima shift to somewhat lower temperatures and decrease markedly in intensity, which sets a strict limit on further improvements in resolution. It should be noted that for the similar Ag/Re(0001) system, such a fourth TDS state could indeed be resolved [10]. Some copper TD spectra from Re(0001) were already published some years ago by He and Goodman [16] and Rodriguez et al. [19]. However, only the β_1 and β_3 states were reported in this work (probably because of insufficient spectral resolution), and no line-shape analysis was carried out.

A central point in metal-on-metal epitaxy is the determination of the growth mode of the deposited material. Although the electron spectroscopies XPS and AES are particularly suited to shedding light on this particular property (see Sections 3.3 and 3.4), TDS can also contribute useful information here, i.e. by following the (layer-dependent) monolayer saturation coverages. An example was recently given in our Ag-on-Re(0001) work [10], in which we could monitor differences in the monolayer coverages of a few per cent between the first and the second Ag monolayer, and hence establish evidence of pseudomorphic growth exclusively for the first monolayer. As we showed in this work, the so-called *layer plot* representation of the TDS data suggested by Schlichting and Menzel [29] is especially helpful to extract this information from standard TDS data. To construct a layer plot, the 'ordinary' TD spectra (an example of which is given in Fig. 1) are integrated from right to left up to a given temperature T_f. In this way, the remaining deposit material is determined according to the expression:

$$\Theta_{res} = \frac{1}{\beta} \int_{T_\infty}^{T_f} p \, dT. \quad (1)$$

For each such temperature T_f, the desorption rate R (ordinate) is taken and plotted against Θ_{res}. A short comment is necessary as regards the use of the symbol Θ_{res}. Although it definitely represents a *coverage*, there is a difference with respect to the 'static' coverage that describes the (time-independent) surface concentration of deposited material. Θ_{res}, on the other hand, is rather a 'dynamic' quantity, it occurs in TDS experiments only and is time-dependent in that it becomes continuously smaller as the (linear) TDS program proceeds, beginning from the initial coverage Θ_0, and ending with coverage zero.

Note that in a layer plot the desorption occurs from *right to left*, the temperature no longer appears as an independent variable. For strict zero-order desorption kinetics (as is the case with noble gas desorption [29]) there occurs a sudden, i.e. almost perpendicular, break-down of the desorption rate *for all TD traces* as the respective layer population is exhausted. Accordingly, the minimum associated with the depletion of an individual deposit layer is sharp and remains coverage-independent.

For the Cu/Re(0001) system, we reproduce the layer plot as Fig. 2, the curves have been constructed from the TPD spectra of Fig. 1. Clearly, the desorptive contributions from the first and the second layer are more or less separated, while the desorption from the second layer and the multilayers appears merely as a saddle point. Due to the proximity of the strong second-layer contribution and, more importantly, because of the deviation from the strict zero-order desorption kinetics near the transition from first to second monolayer, there is no common break-down in the desorption rate as the first and second layer, respectively, become depleted. Therefore, the position of the

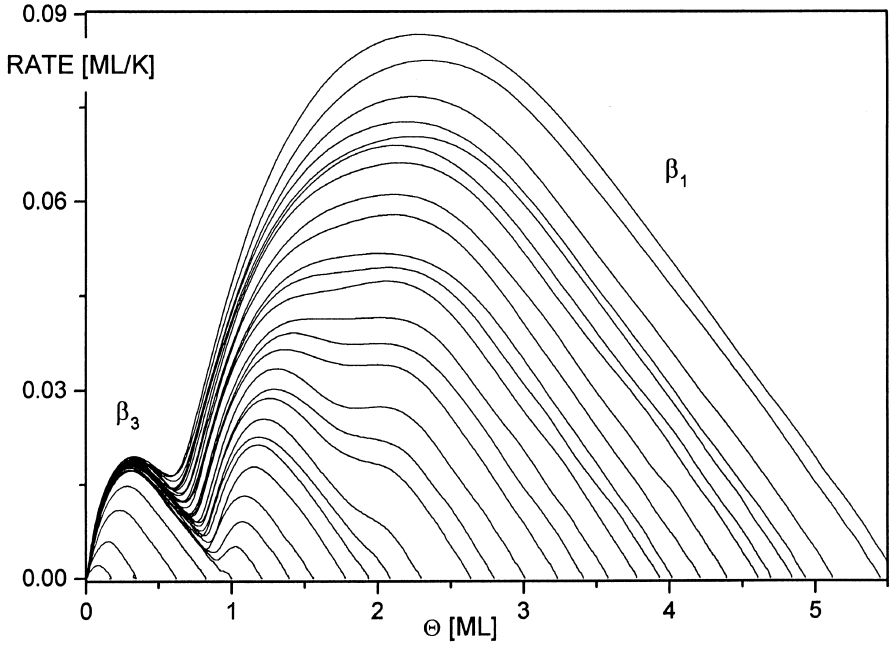

Fig. 2. Layer plots for the TD spectra displayed in Fig. 1. The parameter of the curves is the initial coverage, Θ_0. Note that the temperature (which is an implicit parameter only) rises from right to left! See text for further details.

'depression' between the contributions of the first and second layer decreases fairly strongly with increasing Cu coverage, and a definite conclusion about a coverage dependence of the monolayer population cannot be drawn, in contrast to the Ag-on-Re(0001) system [10]. The only safe observation is that there occurs a *continuous* shift of the minimum in the layer plot, i.e. no abrupt change in the slope can be seen as was the case with Ag. The *absence* of such an effect here only indicates that the Cu growth within the first bilayer largely differs from the Ag growth on the same surface, a fact which is by no means surprising in view of the dissimilar atomic diameters of Cu and Ag. Next, we turn to the analysis of the energetics of desorption.

The basis for any evaluation of the kinetic and/or energetic parameters from a TPD experiment is the Polanyi–Wigner equation:

$$\text{desorption rate } R \equiv \left|\frac{\mathrm{d}\Theta}{\mathrm{d}T}\right| = \frac{\nu_x}{\beta}\,\Theta^x \exp\left(-\frac{\Delta E^*_{\mathrm{des}}}{kT}\right), \tag{2}$$

Θ being the Cu coverage, ν standing for the pre-exponential factor, β for the heating rate, and $\Delta E^*_{\mathrm{des}}$ representing the activation energy for desorption (we choose the notation $\Delta E^*_{\mathrm{des}}$ independent of the interesting physical question of whether or not the desorption process really is an *activated* phenomenon in the kinetic sense). In order to specifically determine $\Delta E^*_{\mathrm{des}}$ and ν for the first two Cu layers on the Re(0001) surface, we measured a TPD series just in this coverage range $0 \le \Theta_{\mathrm{Cu}} \le 2.1$ ML. The resulting spectra are shown in Fig. 3 and clearly contain only the β_3 and the β_2 state. Especially for higher initial coverages, the leading edges of both states fall together (however, only up to a distinct temperature limit, T_g, see Section 4). This behavior is indicative of a zero-order desorption process, whereby the desorption kinetics imply a homogeneous desorption rate that rises exponentially with temperature, *independent* of the surface concentration of deposited Cu. Ideally, the TPD maxima (associated with the different initial coverages Θ_0) should be located directly on the leading-edge curve. (Systematic

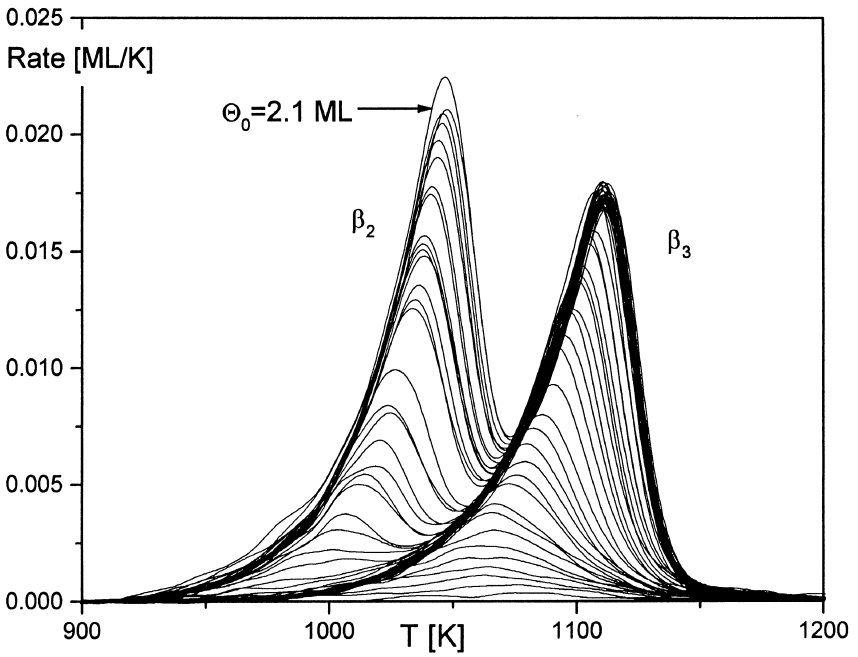

Fig. 3. Series of Cu thermal desorption spectra from Re(0001) for the coverage range $0<\Theta<2.1$ ML displaying the β_3 and β_2 desorption states. The heating rate was again 7.7 K/s, the deposition temperature 673 K.

deviations from this ideal behavior allow conclusions on certain details of the desorption reaction: a closer view of our TD spectra reveals indeed that in a certain coverage range the desorption maxima appear at a distinct higher temperature than predicted by a single exponential rate law, and we will return to this point in Section 4.) Genuine zero-order kinetics (as observed for the β_1 state) mostly result from a direct transfer of condensed material to the gas phase, caused by a true evaporation or sublimation process. Setting in Eq. (2) the reaction order $x=0$ one immediately obtains a *single*, Θ-independent, exponential rate law. A respective semi-logarithmic plot for the coverage range $0.30\leq\Theta_{Cu}\leq2.0$ ML yields an activation energy for desorption ΔE^{*}_{des} of 320 kJ/mol (which is a little lower than the tabulated heat of Cu sublimation ΔH_{sub} of 334 kJ/mol [35]).

If we assume for the moment a *homogeneous* Cu bilayer, followed by the growth of rather three-dimensional crystallites ('pseudo'-Frank–van der Merwe growth or 'quasi'-Stranski–Krastanov growth), then the particular morphology of the bilayer (and the multilayers) is responsible for the observed zero-order kinetics. So far our assumption primarily rests on previous results for the analogous system copper on a *ruthenium*(0001) surface [23], where just this pseudo-Frank–van der Merwe growth was reported. On the other hand, a STM study to verify the specific growth behavior of the Cu-on-Re(0001) system is presently under way [26]. We simply note that the assumption of a pseudo-Frank–van der Merwe growth for Cu/Re(0001) is not in contradiction with our AES and XPS [36,37], as pointed out further below.

Somewhat more difficult is the situation in the submonolayer coverage regime. As with the Ag-on-Re(0001) system [10], there is evidence of a two-dimensional phase equilibrium also with the Cu deposit. This equilibrium precedes the actual thermal desorption reaction step and concerns a transition between a diluted two-dimensional Cu gas phase and a two-dimensional condensed phase in the form of Cu islands. In other words, a Cu atom embedded in the interior of such an island must first transform to the 2D vapor state before it can

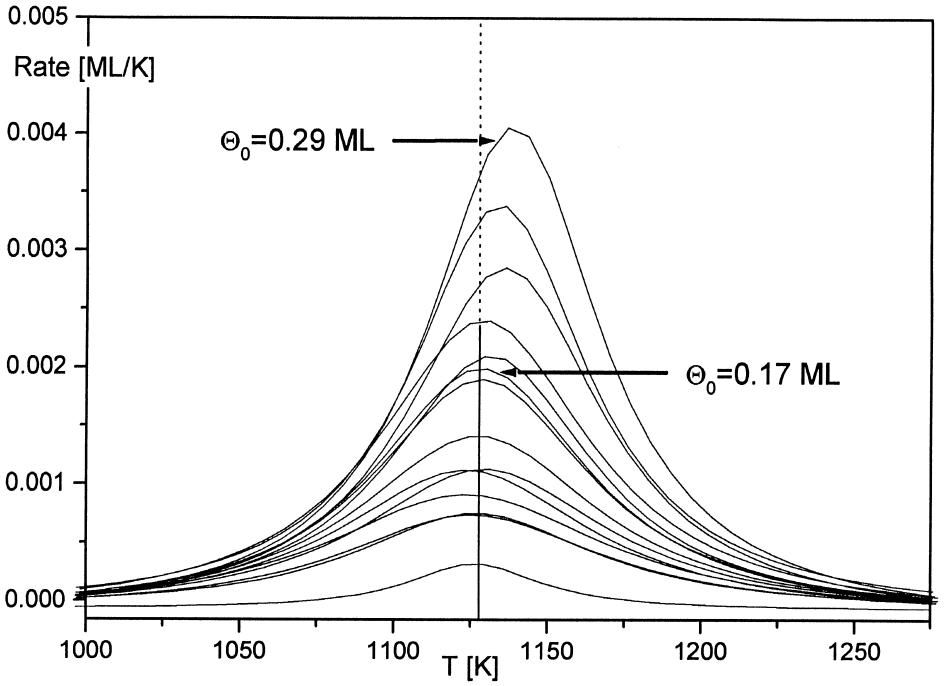

Fig. 4. Series of Cu TDS spectra for the very low coverage range $0<\Theta<0.3$ ML. Heating rate 21.7 K/s; deposition temperature 673 K. Note the practically coverage-invariant temperature position of the β_3 desorption maximum.

leave the surface via thermal desorption. This behavior should especially affect the desorption kinetics in the submonolayer coverage range. We have, therefore, scrutinized the very low coverage regime ($0\leq\Theta\leq0.3$ ML) and taken TD spectra which are shown in Fig. 4. In order to intensify the (small) TDS signals, a fairly large heating rate, $\beta=21.7$ K/s, has been chosen. In contrast to most of the TDS traces of Figs. 1 and 3, the spectra do not have a common leading edge, and hence do *not* follow zero-order kinetics any more. Rather, the TDS maxima remain almost constant at $T=$ 1127 K, indicating rather *first-order* reaction kinetics. This holds strictly for coverages up to $\Theta=$ 0.15 ML and becomes effective also in the course of the TDS runs whenever Θ_{res} reaches this value. First-order kinetics are entirely compatible with the aforementioned assumption of a phase equilibrium between 'solid' Cu islands and two-dimensional Cu gas [27,28], hence we attribute the change in reaction order between $0.1<\Theta<0.3$ ML to this phase equilibrium.

A quite convenient means to analyze the overall desorption kinetics over a fairly large coverage range is provided by a suitable (i.e. isothermal) plot of the Polanyi–Wigner equation [Eq. (2)]. Its logarithm form states:

$$\ln R = x \ln \Theta + \ln \frac{\nu}{\beta} - \frac{\Delta E^{*}_{des}}{kT_{iso}}. \quad (3)$$

Evidently, the slope of the double-logarithmic curve indicates directly the order x of the desorption reaction. A respective 'order plot' [i.e. ln(rate) vs. $\ln \Theta_{Cu}$ for constant temperature T_{iso}] reflects this quantity in a straightforward manner and is shown in Fig. 5 for the coverage range $0\leq\Theta_{Cu}\leq\sim5$ ML. The respective 'isotherms' span a temperature interval from 990 K (bottom curve) to 1130 K (top curve) and differ with regard to the filling of the individual desorption states. At the highest temperatures, merely β_3 is populated, while at the lowest temperature all β states contribute. If we focus on the six or seven bottom 'isotherms' taken in the temperature interval $990\leq T\leq1050$ K, roughly four different sections

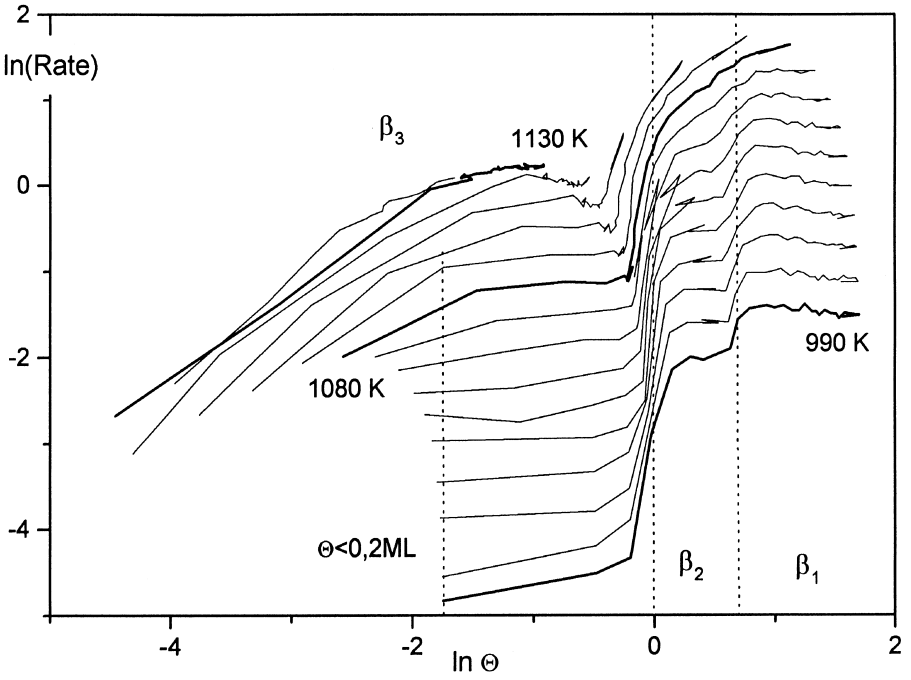

Fig. 5. Order plots of the TPD spectra of Fig. 1, based on Eq. (3). Plotted is the logarithm of the desorption rate versus the logarithm of the Cu coverage that is still present on the Re surface. The individual curves have been constructed for isothermal conditions, i.e. the temperature is a parameter. See text for more details.

with a distinct slope and hence desorption order x can be distinguished. There are three sections with slope zero which are easily associated with the (highly populated) β_3, the (second-layer) β_2, and the (multilayer) β_1 state. Quite nicely, the transition from zero-order kinetics (slope 0) to first-order kinetics ($\rightarrow$slope 1) can be visualized in all 'isotherms' as the coverage falls below $\Theta = 0.3$ ML.

While the analysis of the desorption kinetics yields information about the desorption mechanism, the determination of the activation energy for desorption and the pre-exponential factor calls for a more sophisticated analysis. The established procedures by King [31] or Bauer et al. [32] were already mentioned. Here we would like to add a few remarks on the details of how we conducted our computer-aided analysis through the TPD data.

According to Eq. (2), the rate R of a (temperature-programmed) thermal desorption process is a function of two variables, i.e. temperature T and momentary adsorbate coverage Θ_{res} (which itself is a function of the temperature). If we control T and measure R, the coverage is automatically adjusted by the system, but it can be evaluated only *after* the TDS experiment has been carried out. Actually, the desorption rate R is a (bent) trajectory in T, Θ_{res} phase space. Parametrization of one of these variables then leads to relations for the isothermal (T=constant) or isosteric (Θ_{res}=constant) desorption. Note, however, that neither true isothermal nor isosteric conditions prevail in a 'normal' TPD experiment.

Nevertheless, it is possible (with some effort though) to conduct a real *isothermal* desorption experiment as was shown some time ago by Pavlovska et al. [38]. These authors indeed kept their sample at a constant temperature (where desorption occurs), but they simultaneously deposited film material so as to reach a true equilibrium situation. At time $t = 0$ the vapor flux was suddenly stopped and the subsequent isothermal desorption followed and measured.

A real *isosteric* desorption experiment cannot

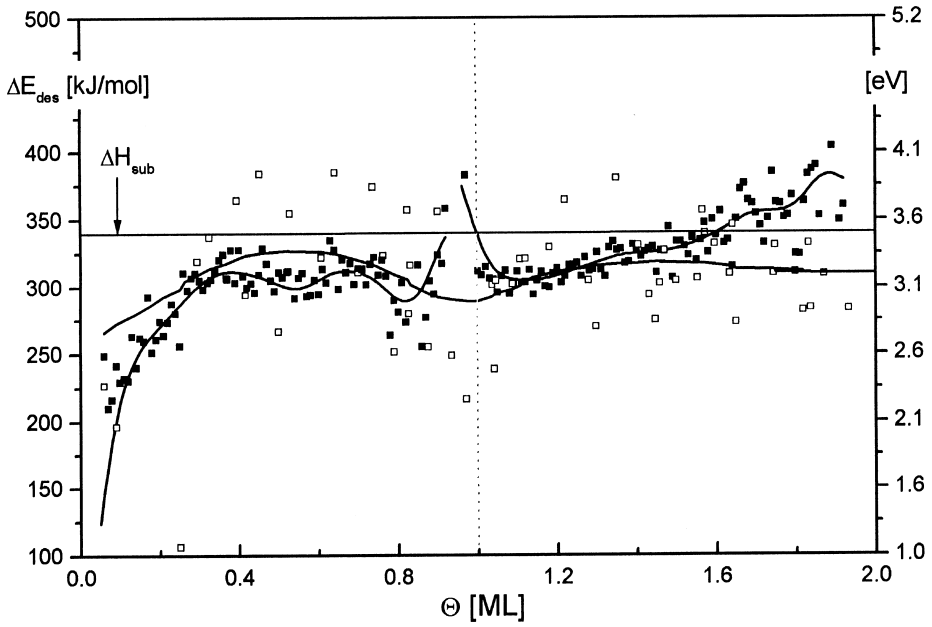

Fig. 6. Activation energies for desorption, ΔE^*_{des}, as a function of the Cu coverage, Θ_{Cu}. The data points were evaluated by two different methods. The filled squares denote the data obtained from the 'total' analysis suggested by Bauer et al. [32], the open squares refer to the threshold analysis introduced by Habenschaden and Küppers [33]. Also indicated in the figure is the heat of sublimation of bulk Cu as a horizontal line.

be carried out, rather, various TD spectra have to be measured and integrated for certain narrow temperature intervals. From each TDS trace, a pair of definite Θ_{res} and corresponding rate R (R will be different for each Θ_{res}) must be taken, plotted in a suitable manner and evaluated according to Eq. (2). Following the suggestion by Bauer et al. [32], it is convenient to first define the lifetime τ (Θ) of the adsorbate as the ratio between the actual coverage Θ_{res} and the corresponding rate R:

$$\tau(\Theta)=\frac{\Theta_{res}}{R}=\tau(\Theta, T). \tag{4}$$

One then obtains new triples of values for T, $\tau(\Theta)$, and Θ, and upon rearranging Eq. (1) and taking the logarithm, Arrhenius-type plots can be constructed:

$$\ln \tau(\Theta)=f\left(\frac{1}{T}\right)=-\frac{\Delta E^*_{des}}{k_B T}+\ln\frac{\beta}{\nu}, \tag{5}$$

whose slope yields immediately the activation energy for desorption, ΔE^*_{des}, for the associated Θ_{res}, averaged over a certain temperature interval. Repeating this procedure for various values of Θ_{res} finally yields the coverage dependence of the activation energy of desorption, $\Delta E^*_{des}(\Theta)$. This so-called total analysis gives access to quite accurate data, provided a dense series of TPD spectra is available. Another possibility of getting access to ΔE^*_{des} was suggested by Habenschaden and Küppers [33]; a plot of $\ln R$ against the inverse temperature yields the activation energy for desorption relatively accurately, provided only the initial part of a desorption trace is subjected to the analysis. We have applied various analyses to our data and obtained the coverage dependence of ΔE^*_{des} reproduced in Fig. 6. We note that the different analyses nevertheless yield relatively similar energies, which imposes some reliability on our data. Starting at very low Cu coverages we note that between $0 \le \Theta_{Cu} \le 0.25$ ML there is a pronounced increase of ΔE^*_{des} from ca. 200 to roughly 300 kJ/mol. This fairly strong increase is usually explained by attractive mutual interactions

between the adatoms, and reflects the tendency of Cu island formation. This behavior implies that Cu atoms arriving from the gas phase will find more favorable bonding conditions at an already existing Cu oligomer than an isolated Cu particle on the flat Re surface.

Between $0.25 \leq \Theta_{Cu} \leq 0.75$ ML, ΔE^*_{des} remains practically constant at a level of ~ 310 kJ/mol, whereby this constant level is influenced by the aforementiond phase equilibrium 2D gas phase–2D 'solid' islands. The value of the desorption energy is somewhat smaller than the characteristic heat of Cu sublimation (see above), because the Cu atom first transforms to the 2D gas state (in which it is much less coordinated than in the 3D bulk), and removal of this atom into the gas phase requires less energy effort.

Interesting features are encountered in the coverage range close to the filling of the first monolayer, i.e. in the interval $0.75 \leq \Theta_{Cu} \leq 1.1$ ML. Bauer's method yields first a rapid decrease by ~ 20 kJ/mol and a subsequent increase of ~ 80 kJ/mol, until at $\Theta_{Cu} = 1.0$ ML the energy value has returned to ~ 310 kJ/mol. We note that quite a similar effect has been described for the Cu-on-W(110) system by Bauer et al. [1]. Neglecting the (theoretical) possibility of a systematic error caused by overlapping states, we attribute it to a real physical (morphological) effect. Close to the monolayer coverage, the Cu atoms are packed quite densely, and because of the misfit any registry with the Re substrate is lost. Recall that the Cu atom is somewhat smaller than the Re atom and, accordingly, as many Cu atoms as Re surface atoms (1.5147×10^{19} m^{-2}) should easily be accommodated. However, if the Cu atoms tend to build up their own lattice, then the Cu overlayer would contain 1.7745×10^{19} m^{-2}, corresponding to a $\sim 17\%$ larger density, and the registry with the Re(0001) surface must be given up. Consequently, misfit-induced strain is expected which may reduce the overall Cu binding energy to the Re substrate. However, as soon as the second layer begins to form, attractive interactions between the Cu atoms of the second layer (leading to the formation of Cu islands) may cause a re-increase of the adsorption energy, until finally the characteristic cohesive energy of the Cu bulk is reached. Turning to the coverage dependence of the desorption energy within the second Cu layer, we note a slight increase of ΔE^*_{des} from ~ 310 to ~ 340 kJ/mol. While in principle strongly Θ-dependent restructuring effects of the Cu bilayer are conceivable in this coverage range, the observed features (cf. Fig. 3) do not resemble those reported recently for the system Ag-on-Re(0001) [10] and mentioned above, and sudden restructuring effects are rather unlikely. It seems as if the interactions probed for the bilayer by the TPD experiment predominantly reflect the binding of Cu atoms to the other Cu neighbor atoms; these second layer atoms no longer have excessive chemical contact with the topmost atoms of the Re substrate, and the lattice misfit is overcome *gradually*, i.e. additional Cu atoms are incorporated here and there in the first layer and in the second/third layer until finally a more or less 'perfect' Cu(111) lattice is reached. Accordingly, the measured activation energy for desorption of 340 kJ/mol is practically identical with the Cu heat of sublimation (341 kJ/mol [35]). This tendency is also reflected in the zero-order desorption kinetics which are characteristic for desorption from the multilayer regime.

The data analysis also yields the frequency factor for the desorption process as a function of the coverage. As can be seen from Fig. 7, $\nu(\Theta)$ follows the Θ-dependence of the desorption energy in every detail, which may be taken as a hint to the operation of a massive compensation effect. Quite a similar behavior was recently observed in our study of the Ag-on-Re(0001) system [10]. Among others, the frequency factor reflects the entropy of the adsorbate system. Close to the filling of the monolayer the configurational entropy is expected to reach a minimum value, because most of the Cu atoms are localized on the Re surface. However, as the transition to the second Cu layer takes place, the few Cu atoms residing in the second layer at still small coverages possess quite a large configurational entropy, thus explaining the increase of $\nu(\Theta)$ around $1.0 \leq \Theta_{Cu} \leq 1.1$ ML.

3.2. Low-energy electron diffraction

Copper deposition at 300 K up to a coverage of $\Theta = 0.8$ ML makes the Re(1×1) LEED spots somewhat diffuse and introduces a slightly

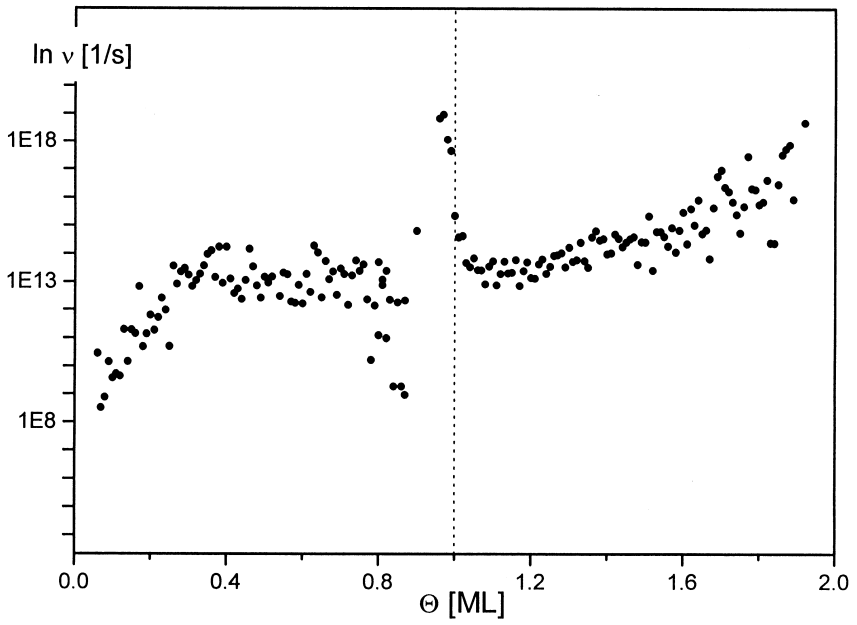

Fig. 7. Frequency factor ν as a function of Cu coverage Θ as determined by the total analysis suggested by Bauer et al. [32]. A comparison with Fig. 6 immediately reveals that the function $\nu(\Theta)$ follows the coverage dependence of the activation energy for desorption, $\Delta E^{*}_{\mathrm{des}}$, in every detail, suggesting a pronounced compensation effect.

increased uniform background. No Cu-induced 'extra' spots are visible, even after prolonged annealing at 970 K. However, as the coverage is increased to beyond $\Theta = 0.8$ ML, new Cu-induced diffraction features become visible and remain stable up to $\Theta \simeq 2$–3 ML. The respective LEED pattern is reproduced as Fig. 8. Six satellites surround the Re(1×1) spots at a distance which is roughly 1/14 of the reciprocal Re lattice vector; the respective vectors of the Re and Cu sublattices are parallel. A 10 min anneal at 970 K greatly improves the long-range order of the (14×14) superstructure in that now also the second and third order diffraction spots become clearly visible. (All other fractional-order LEED spots remain, however, invisible because of their weakness.) Nevertheless, these LEED features clearly suggest that especially for $\Theta > 0.8$ ML, the Cu atoms form a more or less homogeneous layer or at least large homogeneous islands which exhibit the characteristic copper lattice constant and are directed parallel to one of the main symmetry directions of the hexagonal Re lattice ($[1\bar{2}10]$ direction). In this coincidence structure, a string of 15 Cu atoms

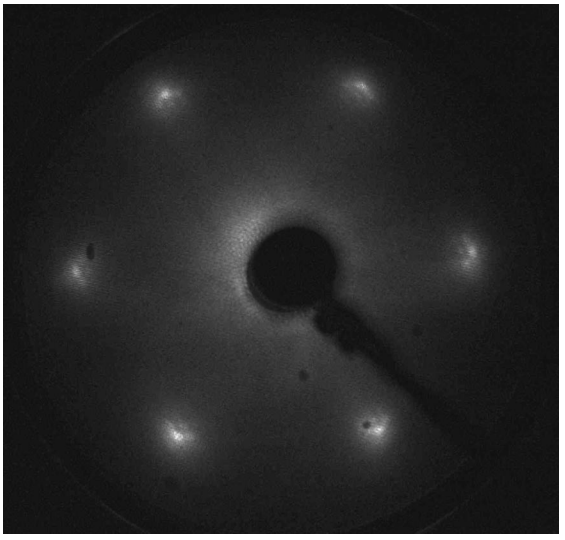

Fig. 8. Reproduction of the LEED pattern showing the (14×14) superstructure formed by a $\sim$2 ML Cu coverage at 673 K. Only the first and (much weaker) second-order fractional beams are recognizable. The electron energy was 126 eV.

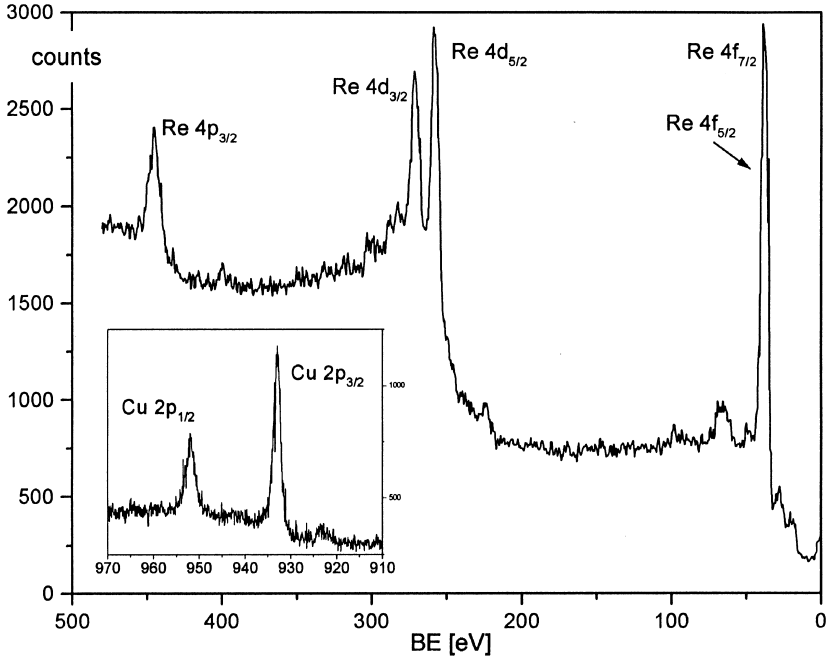

Fig. 9. Survey X-ray photoelectron spectrum obtained with a 6 ML Cu film deposited onto the Re(0001) surface at 300 K. Shown are the core levels of the Cu $2p_{3/2}$ and $2p_{1/2}$ (inset) and the Re $4f_{5/2}$ and $4f_{7/2}$ as well as the Re $4d_{3/2}$ and $4d_{5/2}$ electrons. Further details can be taken from the text.

matches a string of 14 Re atoms, that is, every 14 Re atoms a Cu atom can occupy a Re 'site' with identical coordination. This should lead to a slightly, but periodically, undulated Re–Cu bilayer which is believed to be responsible for the observed LEED superstructure. It is evident from Fig. 8 that the fractional spots with higher order are particularly well visible in the $[10\bar{1}0]$ direction, which means that the long-range periodicity (and hence the undulation) occurs preferably in this direction of the Re lattice. This could be caused by a non-uniform terracing of the Re surface leading to fairly wide terraces and a particularly regularly undulated Cu film just along the $[10\bar{1}0]$ direction.

As the Cu coverage is further increased to $\Theta \geq 5$ ML, the fractional-order beams disappear again and are replaced by a genuine hexagonal (1×1) LEED pattern. By comparison with the clean Re(1×1) structure, all lattice vectors are by a factor $15/14 = 1.071$ larger, as expected for the growth of fairly thick genuine Cu(111) crystallites whose diffraction features no longer interfere (at least not at the electron energies used) with those of the Re host lattice. The relatively low background thereby indicates a reasonable long-range periodicity of these crystallites.

3.3. X-ray photoelectron spectroscopy

In order to learn more about the electronic interaction between the adsorbed Cu atoms and the Re substrate and to further characterize the growth behavior of the Cu films, we performed XPS measurements with Cu films of various thicknesses that were deposited at room temperature. We studied particularly the Re 4d and 4f and the Cu 2p core levels with respect to intensity and energetic position.

The survey spectrum of Fig. 9 spans the energy range up to $\sim$500 eV and displays the spin–orbit split Re core level excitations, while the inset covering the energy range between 910 and 970 eV shows the spin–orbit split Cu $2p_{1/2}$ and $2p_{3/2}$ core

levels. The Cu coverage in this experiment was approximately 6 ML. A challenging problem in heteroepitaxy concerns the electronic interaction between guest and host metal. For chemical systems which strongly interact at the common interface, more or less pronounced changes in electron binding energies are expected (*surface chemical shifts*). To scrutinize this interaction between Cu and Re we monitored the energetic positions of the Cu $2p_{3/2}$ and the Re $4f_{7/2}$ and $4f_{5/2}$ doublet as a function of Cu coverage, whereby Θ_{Cu} was extended up to 10 ML. The results are shown in Fig. 10. Within the limits of our resolution, practically no chemical shift is detectable, neither for the Cu nor for any of the Re core levels. This underlines the apparently very weak chemical interaction between Cu and Re (which is expected from the comparable electronegativities of the two elements [11] as mentioned above). We mention that quite a similar conclusion has been drawn previously by Rodriguez et al. [19] who located the Cu $2p_{3/2}$ core level at 932.75 eV for $\Theta \leq 1$ ML, but at 932.90 eV at 20 ML. The resulting shift in electron binding energy of 0.15 eV was considered vanishingly small compared to Cu on Rh(100) or on Ru(0001).

Conclusions on the growth mode of the Cu deposit can be drawn from graphs in which both the deposit and substrate XPS signal intensity, respectively, is plotted as a function of the deposited amount, i.e. the Cu coverage Θ_{Cu}. For this purpose, we have integrated the Re and Cu XPS signals, subtracted the background signal, and plotted the resulting intensities against the Cu

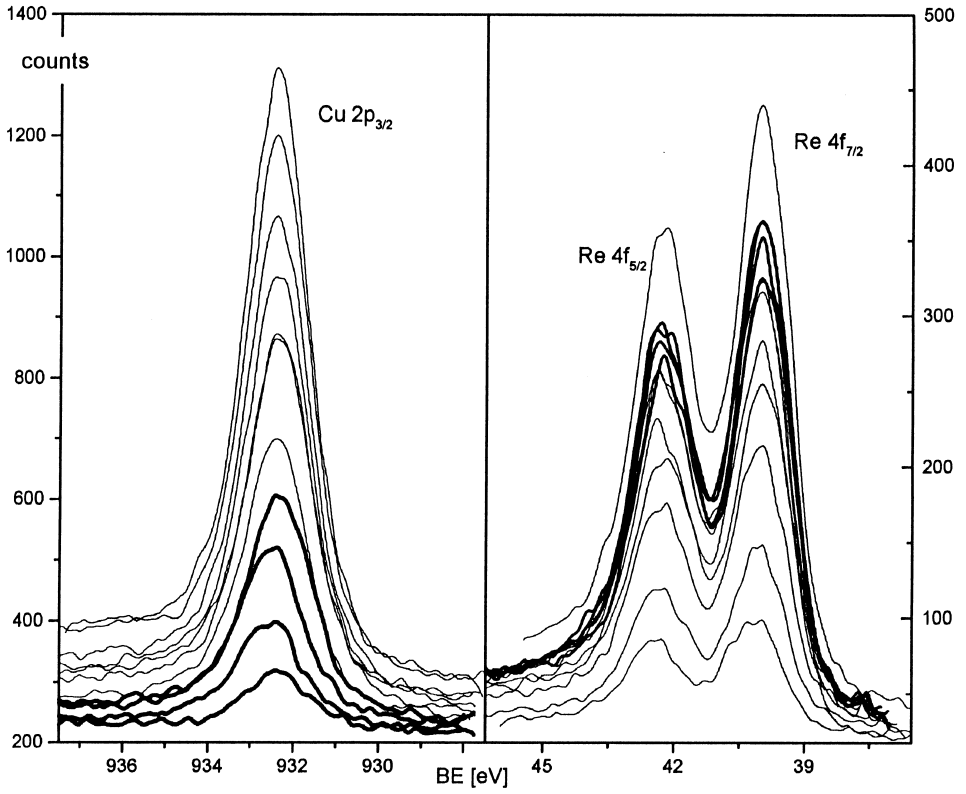

Fig. 10. Detailed XP spectra displaying the energy range between 930 and 940 eV (Cu $2p_{3/2}$ and $2p_{1/2}$ doublet) and between 40 and 50 eV (Re $4f_{5/2}$ and $4f_{7/2}$ core electrons). The constant, coverage-invariant position of the core level excitation indicates a negligible chemical interaction between host and guest metal in agreement with previous conclusions [19]. In the legend, we have indicated the coverage and have, in addition, marked the first monolayer curve by a bold line.

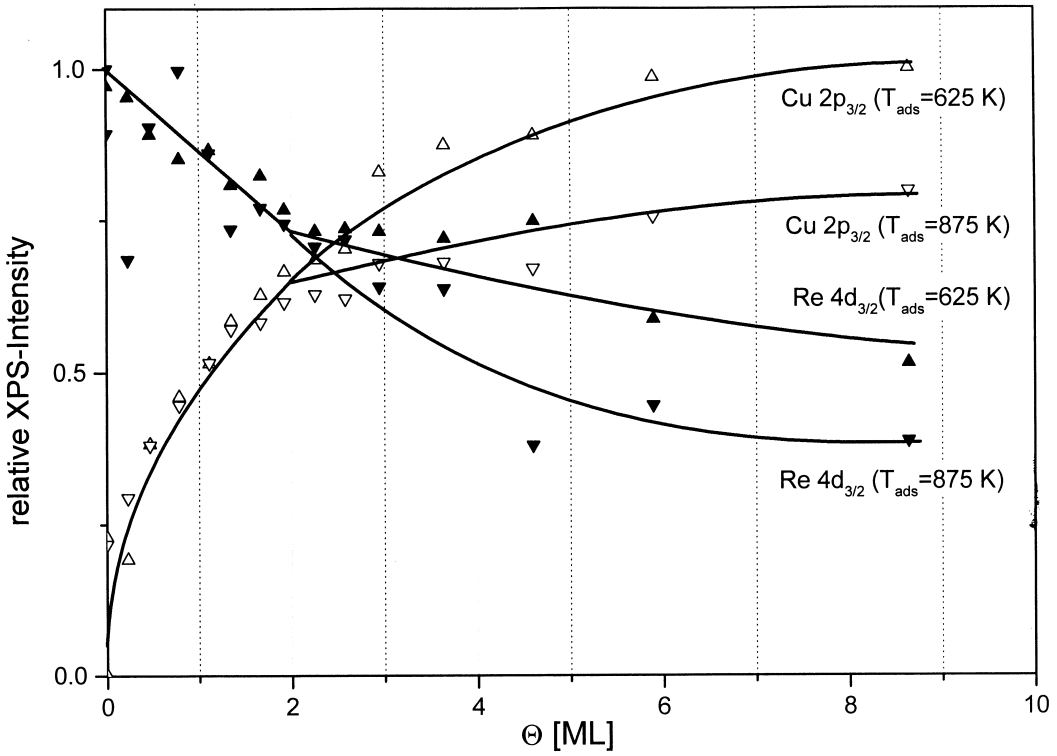

Fig. 11. Plot of the integrals of the XP signals as a function of the overall Cu coverage (determined by TPD). The data were obtained from two different Cu films deposited at 625 K (up triangles) and 875 K (down triangles). The filled triangles refer to the Re $4d_{3/2}$ and $4d_{5/2}$, the open triangles to the Cu $2p_{3/2}$ and $2p_{1/2}$ excitations. Note that only the high temperature curves exhibit a sharp bend at $\Theta_{Cu}=2$ ML.

coverage; the curves shown in Fig. 11 were obtained. This figure contains data of Cu films prepared at two different temperatures, i.e. at 625 K and 875 K. Regardless of the deposition temperature, all curves exhibit a steady increase of the Cu (decrease of the Re) signal intensity within the coverage range of the first two monolayers, i.e. between $0<\Theta_{Cu}<2$ ML. The relatively pronounced scatter of the data points does not allow a very detailed analysis of the growth mode in this coverage range, but one can clearly realize that all curves level off for coverages $\Theta_{Cu}\geq 2$ ML. As Θ_{Cu} approaches 8 to 10 ML, the Cu signal intensity seems to saturate, regardless of the temperature, and also the Re signal remains practically constant, however, not on a zero level, but with a 30% intensity of its initial value. In other words, the Re substrate remains 'visible' even after deposition of fairly large amounts of Cu. This is another hint to the quite 'open' structure of the Cu film, especially at elevated temperatures which allows Re core level electrons to escape through the deposited Cu film. While the features described above practically do not exhibit any temperature effect below $\Theta_{Cu}=2$ ML, such a dependence comes into play for coverages $\Theta_{Cu}\geq 2$ ML. The Cu 875 K curves are way down compared to the corresponding 625 K data. Interestingly, the respective Re signal intensities obtained after high-temperature deposition and/or annealing also drop to below the room temperature values.

The overall growth behavior can be interpreted as reflecting a pronounced Stranski–Krastanov type of growth with two first, almost closed, Cu layers on top of the Re surface, onto which rather three-dimensional Cu crystallites form. The peculiar temperature dependence of the intensity versus Θ_{Cu} relation provides further hints to certain

details of (thermally activated) Cu diffusion and redistribution processes. First of all, there is no effect of annealing on the intensity–coverage relation for the first two Cu monolayers. This behavior indicates a preferably two-dimensional distribution of the Cu bilayer regardless of the temperature. As soon as Θ_{Cu} exceeds 2 ML, the high-temperature curves are considerably flatter than the low-temperature data. We argue that fairly open (possibly dendritic) two-dimensional Cu islands form at lower temperatures, while deposition or annealing at elevated temperatures forces the Cu atoms of the third and following layers to transform to rather three-dimensional aggregates. In other words, only the degree of dispersion of the Cu deposit is temperature dependent. From our data and in view of the results obtained with the related Cu-on-Ru(0001) system [22–24], we assume the formation of fairly rough films on top of the flat Cu bilayer at room temperature, with a relatively large emitting Cu area that gives rise to more or less intense XP signals. At the high deposition or annealing temperature the Cu atoms gain a higher mobility and can redistribute. Consequently, rather more compact three-dimensional Cu pyramids will form via diffusion, thus producing increasing areas of 'thin' Cu bilayers through which the escaping Re photoelectrons are less effectively attenuated, while the attenuation of Cu core level electrons emitted from the bottom layers within a pyramid is quite marked.

3.4. Auger electron spectroscopy

The XPS data are entirely confirmed by our AES investigations. We followed the peak-to-peak amplitudes of the Cu $M_VN_IN_{II,III}$ and the Re $N_{VI,VI}O_{IV,V}O_{IV,V}$ Auger transitions at 62 eV and 33 eV, respectively, as a function of the Cu coverage and obtained Fig. 12. The choice of similar

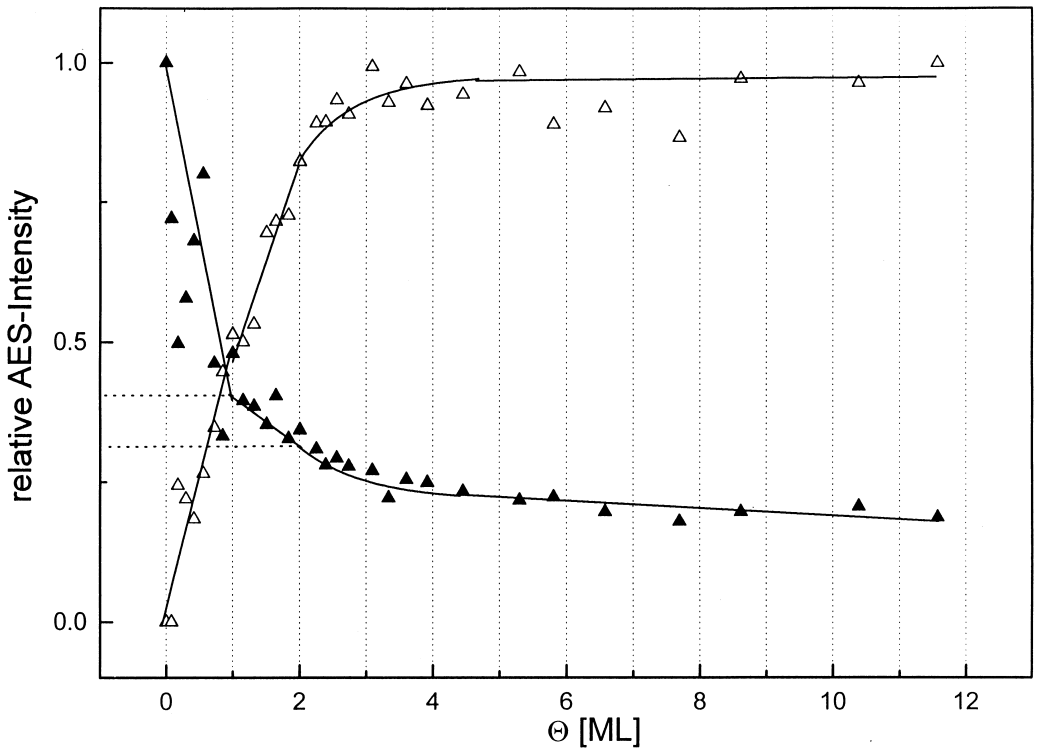

Fig. 12. Plot of the Cu $M_5N_1N_{2,3}$ Auger signal intensity at 62 eV and the respective Re $N_{6,7}O_{4,5}O_{4,5}$ intensity against the Cu coverage (ML). The data refer to a deposition temperature of 673 K and resemble the XP data reproduced in Fig. 11. See text for details.

Auger electron energies ensures that the depth information is restricted to the first two to four atomic layers. However, the principal features of Fig. 12 do not change, when we take the Cu $L_{III}M_{IV,V}M_{IV,V}$ and the Re $N_VO_{III}O_{III}$ Auger transitions at 930 eV and 176 eV, respectively. A first steep linear increase of the Cu and a related decrease of the Re signal intensities in the submonolayer range $0<\Theta_{Cu}<1$ ML is followed by another linear increase (decrease) with a somewhat reduced slope in the bilayer coverage range $1<\Theta_{Cu}<2$ ML. Thereafter the Cu signal intensity levels off fairly abruptly, while the Re intensity remains constant on a ca. 30% level of the initial intensity of the Cu-free Re surface as Θ_{Cu} approaches $\sim$4 ML; it decreases to a final value of $\sim$20%, after deposition of altogether 12 ML. We explain the fact that the Cu Auger signal remains practically constant for $4<\Theta_{Cu}<12$ ML by the 'constant' growth mechanism which leads to a fairly 'open' morphology with three-dimensional Cu aggregates. We recall that the conclusions drawn from AES correspond to the situation seen by XPS (cf. Section 3.3). Both sets of data suggest a Stranski–Krastanov type of growth in which three-dimensional Cu clusters form after completion of the first Cu bilayer(s) with fairly rough layers in the unannealed state and rather more compact three-dimensional films after annealing at 870 K.

4. Discussion

In this section, we will first distinguish and discuss the phenomena of *growth and structure* of the Cu films and thereafter expand somewhat on the *energetics and kinetics* of the desorption process, including a detailed comparison with LEED and TDS data that were previously obtained in Goodman's laboratory.

4.1. Growth and structure of the Cu films

One of the central problems in heteroepitaxy is how the deposit material can overcome the lattice misfit, and it is particularly interesting to compare the respective behavior of deposit metals with too small and too high atomic diameter, respectively, to match the lattice spacings of the (rigid) host metal. In our two studies dealing with Ag and Cu film growth on a Re(0001) surface, we have addressed this problem: Cu is by $\sim$8.2% smaller, Ag $\sim$4.6% larger than a Re atom. Bauer [39] pointed to certain limitations for 'oriented' growth of lines of atoms on bcc (110) substrates and compared the atomic radii of deposited film, r_f, and substrate metal, r_s, according to the relation $(r_f-r_s)/r_s=\Delta r/r_s$. He states that a misfit of -9.1% for Ni/W(110) and $+1.2\%$ [example Pt/W(110)] can be tolerated for the growth of linear (1D) chains. For two-dimensional arrays of atoms (equivalent to pseudomorphous growth) basically similar limits should apply (although the detailed numbers may be different). Both Cu and Ag are electron-rich sp-metals with a similar electronic structure (filled d-bands located $\sim$3 eV below the Fermi level), while the Re(0001) surface with its extraordinarily high surface free energy can be considered sufficiently rigid that it will presumably not alter its geometric structure too much upon adsorption of the noble metal atoms. In view of the high cohesive energy and atomic density of the Re(0001) surface, atom interchange processes as they were reported, e.g. for the Ag films deposited onto a Pt(111) surface [40], must be considered unlikely, although they cannot principally be ruled out. In their AES study of the Cu/Re(0001) system, He and Goodman observed a redispersion effect of a fraction of Cu atoms within 3D Cu clusters and (tentatively) attributed it to possible alloying/dealloying phenomena between Cu and Re [16]. For the Cu/Ru(0001) system — Ru has a relatively similar (somewhat lower) surface free energy as Re — surface atom exchange and or surface alloying processes have been concluded from STM measurements [41].

In several review articles and summaries Bauer has scrutinized the structural problem in heteroepitaxy, with emphasis on noble metal growth on tungsten and molybdenum substrates [1,39,42]. Our Cu and Ag data entirely confirm Bauer's statements that noble metals exhibit attractive lateral interactions and condense in two-dimensional islands (with pseudomorphous internal structure) and do not form phases with long-range

order in the submonolayer coverage range. Actually, quite a similar statement was already made by Neuhaus almost 50 years ago [5]. At low coverages ($\Theta \leq 0.5$ ML) pseudomorphism is frequently observed, for Ag as well as for Cu films. However, as the coverage approaches the full monolayer Cu and Ag behave differently. With Ag (whose diameter has to shrink in order to match the Re lattice and become accommodated in equivalent sites) the pseudomorphous phase remains stable even throughout the monolayer coverage, while the pseudomorphism of the Cu film is destroyed at $\Theta_{Cu} \approx 0.8$–0.9 ML as indicated by a (14×14) pattern. In this coincidence structure the Cu adatoms form a hexagonal close-packed sublattice with the characteristic parameters of a Cu(111) layer. Our respective observation contrasts somewhat with Bauer's conclusion for Cu on W(110), whereafter copper's tendency to form a pseudomorphous layer is so strong that no incommensurate structure has been observed, in spite of the significant strain [41]. One of the reasons for the instability of the pseudomorphous Cu layer on the Re(0001) surface might be the extremely small corrugation amplitude of this surface, 0.1 Å [8], which prevents the Cu atoms from remaining tightly locked in the periodic substrate lattice sites as Θ_{Cu} increases. In addition, attractive lateral (through-bond) interactions between adjacent Cu atoms may be mediated by the Re substrate especially well in this coverage range, leading to islands with the structure of genuine Cu. Up to $\Theta_{Cu} \simeq 0.8$ the Cu film still exhibits a fairly 'open' structure, only as more Cu atoms are deposited can they squeeze themselves into this layer and finally remove the registry with the Re host lattice. Of course, this process will introduce a certain amount of repulsion which should express itself as a decrease in the desorption energy. Actually, such a decrease is indeed observed experimentally, see below. If we have, at this point, a short look at the otherwise similar Ag/Re(0001) system, we note that a (likewise pseudomorphous) Ag film on Re(0001) at a similar coverage will certainly experience much larger repulsive interactions because an Ag atom is somewhat larger than the space provided by a Re surface site.

Bauer remarked [1,39] that the geometric dimensions of guest and host lattice are not the only criteria that govern heteroepitactic growth, another determining factor should be the electronic interaction between the two materials. This is also confirmed by our work. We recall that Ag grows pseudomorphously on Re(0001) up to the monolayer coverage, although then the Ag atoms have to (and indeed do) shrink by several per cent. In other words, they prefer to stay in the adsorption sites of the Re surface lattice despite its small corrugation amplitude and despite the presumably considerable strain energy. Hence, the geometric misfit properties are not a sufficient condition to predict pseudomorphous growth. We must therefore conclude that noticeable differences exist in the chemisorptive interaction between Re and Ag and Cu, respectively, in that Ag interacts somewhat more strongly with Re than does Cu. As pointed out above, also the mediation of indirect lateral interactions between adjacent deposit atoms could affect the film morphology. However, neither with Ag nor with Cu are any core level shifts detectable in our XP spectra, in agreement with observations made by Rodriguez et al. [19] who reported shifts as small as 0.15 eV.

Beyond the monolayer coverage Cu does not grow strictly layer-by-layer. Our data rather suggest that two more or less complete layers are formed on top of the Re surface, before, at coverages $\Theta_{Cu} > 2$ ML, isolated genuine Cu islands of (111) orientation grow. Since the deposition is not performed under conditions of thermodynamic equilibrium, certain kinetic limitations govern the crystal growth, and an incomplete layer growth (Stranski–Krastanov) results, at least at the temperature of 873 K chosen for deposition and/or annealing. If we again compare this behavior with Cu on other refractory metal surfaces, we find quite a similar behavior for Cu/Ru(0001) [20,21,43], Cu/Re(0001) [16,19], Cu/Mo(110) [44,45], Cu/Rh(100) [46], namely, the formation of two (more or less complete) Cu layers, followed by a three-dimensional growth on top of this bilayer.

Concerning the structure of the Cu films in the submonolayer and multilayer range, we first draw attention to He and Goodman's LEED results [16]. They deposited Cu at 115 K. While they did

not find any well-ordered Cu phase in the submonolayer coverage range at this temperature, a whole variety of ordered Cu phases appeared after annealing. Heating of films with $\Theta_{Cu} < 0.2$ ML led to a (2×2) structure with missing beams in the $(m+\frac{1}{2},\ n+\frac{1}{2})$ position and weak 'extra' spots. A sharper $c(2\times2)$ pattern coincided with $\Theta_{Cu} = 0.25$ ML. From the appearance of this (2×2) phase the authors ruled out pseudomorphous growth of Cu in the submonolayer coverage range. On the other hand, they admitted that trace impurities of oxygen or carbon could perhaps be responsible for this structure. Coverages ($\Theta_{Cu} > 0.5$ ML yielded a more diffuse LEED pattern that transformed into a sharp satellite structure (with weak 'extra' spots though) upon annealing to 1073 K. From TPD measurements the authors could attribute these LEED structures to the Cu β_2 state. At 2.2 ML a new Cu-induced LEED structure was reported which the authors designated as a (10×1) phase; annealing at 473 K still changed the features of this structure somewhat; in addition, a hexagonal overlayer with a somewhat larger reciprocal lattice constant formed. The (10×1) phase was explained by an only partially developed Cu superstructure. Still another ordered Cu phase (with a rectangular unit mesh) appeared after deposition of 3.3 ML Cu; it was given the matrix notation

$$\begin{pmatrix} 2 & 0 \\ -\frac{10}{3} & \frac{20}{3} \end{pmatrix}.$$

In addition, again a hexagonal superstructure developed and was particularly pronounced after annealing; this structure was identified as three-dimensional Cu clusters growing in the multilayer coverage regime.

Our re-investigation could not confirm most of the LEED phases described by He and Goodman. In the submonolayer range, we do not find evidence of periodic Cu superlattices which rules out the operation of long-range interactions between the copper atoms (in agreement with Bauer's presumptions [1,39]). Our study rather suggests that only close to the monolayer coverage do the pseudomorphous Cu patches transform to a two-dimensional (1×1) Cu layer. This film tightly covers the Re substrate, thus giving rise to a (14×14) coincidence pattern which likely persists through the bilayer range ($\Theta_{Cu} = 2$ ML) onto which genuine three-dimensional Cu crystallites begin to grow. The respective hexagonal LEED pattern is presumably identical with He and Goodman's hexagonal structure reported for $\Theta_{Cu} \approx 3.3$ ML. (10×1) or rectangular LEED patterns could never be observed, neither in the submonolayer nor in the multilayer coverage range. In the previous study, they may have been produced by traces of carbon, oxygen, or sulfur impurities.

As far as the growth mechanism of the deposited Cu is concerned, we largely agree with the conclusions drawn by He and Goodman. We designate the growth mode as incomplete Frank–van der Merwe or modified Stranski–Krastanov growth, where three-dimensional Cu crystallites form on top of a fairly flat first Cu bilayer. This type of growth seems to be characteristic for Cu films deposited on flat refractory metal surfaces (Ru, W, Mo, etc.) as pointed out above. In this respect, the Cu-on-Re(0001) system behaves as expected.

4.2. Energetics and kinetics of the Cu films

We showed in Section 3 that a careful analysis of TPD spectra can reveal quite a number of details about the energetics and kinetics of the adsorption and desorption process of the deposited material. Again, we have to contrast our results with the data reported previously by He and Goodman [16,19]. They found merely two Cu desorption states β_1 and β_2 with binding energies of 310 and 389 kJ/mol, respectively; any coverage dependence of the activation energy for desorption was not evaluated or taken into account. β_2 was associated with the monolayer coverage ($\Theta_{Cu} = 1.52\times10^{15}$ atoms/cm^2), while β_1 was believed to be due to the multilayer state. As regards the kinetics of Cu desorption, an approximate zero-order was deduced from the *approximate* common leading edge of the TPD low-temperature tails. It was argued that the slight, but apparent, deviations could be caused by a phase equilibrium or by evaporation from 2D islands.

In our investigation we could indeed confirm that the existence of a 2D solid–gas equilibrium in

the submonolayer range greatly affected the shape (and the kinetics) of the Cu desorption states. We were able to resolve a third state in the Cu TPD spectra and could thus work out binding energy differences between the second and third (and all following) Cu layer(s). Furthermore, our detailed TPD line-shape analysis clearly revealed evidence of surprisingly pronounced attractive mutual interactions between the Cu atoms (these are responsible for the Cu island formation at elevated coverages). The desorption energy increases within the first monolayer from $\sim$200 kJ/mol ($\Theta_{Cu}=0.1$ ML) to $\sim$325 kJ/mol ($\Theta_{Cu}=0.8$ ML). For the second-layer state we deduced a similar trend in the desorption energy, which is, however, much less pronounced: ΔE^{*}_{des} increases only from $\sim$330 kJ/mol at $\Theta_{Cu}\approx 1.1$ ML to $\sim 365\pm 20$ kJ/mol at $\Theta_{Cu}\approx 2.0$ ML. The heat of sublimation of Cu, ΔH_{sub}, is tabulated as 341 kJ/mol [35] which means that the desorption energy of the complete second layer is close to the heat of sublimation of bulk Cu, in agreement with the conclusions that three-dimensional clusters of genuine Cu grow on top of the first Cu bilayer.

As far as the desorption kinetics are concerned we could demonstrate that the order of the desorption reaction is strongly coverage-dependent [its behavior resembles very much the Ag/Re(0001) system] and changes from first to approximate zero-order around $\Theta_{Cu}=0.15$ ML, due to the existence of a phase equilibrium 2D condensed–2D gas phase. A forthcoming paper will expand on the details of this phase equilibrium, including a comparison with the similar Ag/Re(0001) system.

The comparison between our TDS data and those published previously by He and Goodman immediately shows that the former analysis was by far too crude to reveal the interesting details of the energetics and kinetics of Cu desorption from the Re(0001) surface.

A final note concerns the electronic interaction between Cu and Re. Here we entirely agree with the statement of Rodriguez et al. [19], who concluded, from the vanishingly small XP core level binding energy shift of merely 0.15 eV, on a negligible 'chemical' interaction between the two elements. On the basis of their practically identical electronegativities any polarization or charge transfer effects at the interface can be safely ruled out. Our TPD data provide no hint whatsoever of any energetic effects that could point to surface alloy formation or site exchange effects. Forthcoming STM measurements to be performed with the Cu/Re(0001) system [26] will provide further information on this issue. In this respect, the Cu/Re(0001) system is expected to behave quite similarly to the previously investigated Ag/Re(0001) system. Work function measurements as a function of Θ_{Ag} revealed that there was a more or less smooth decrease from the initial $\Delta\phi$ value of the Re surface to the lower work function of the Ag film, in the coverage interval of approximately three Ag layers. Although we did not perform $\Delta\phi$ measurements with Cu, we expect quite an analogous behavior, that is to say, a lowering of the work function by several hundred millivolts to the final value of the genuine Cu(111) surface.

Acknowledgements

We gratefully acknowledge financial support of this work by the Deutsche Forschungsgemeinschaft through SFB 290. We are grateful for the technical help of Rudolf Cames and Karin Schubert.

References

[1] E. Bauer, in: The Chemical Physics of Solid Surfaces and Heterogeneous Catalysis Vol. III, Elsevier, Amsterdam, 1984, p. 1.
[2] B.T. Jonker, J.P. Hereman, E.E. Marinero, Characterisation and Properties of Ultrathin Magnetic Films and Multilayers, Materials Research Society, Pittsburgh, PA, 1989.
[3] P. Wissmann (Ed.), Thin Metal Films and Gas Chemisorption, Studies in Surface Science and Catalysis Vol. 32, Elsevier, Amsterdam, 1987.
[4] M. Wuttig, B. Feldmann, T. Flores, Surf. Sci. 331–333 (1995) 659.
[5] A. Neuhaus, Fortsch. Miner. 29/30 (1951) 138.
[6] J.A. Venables, Surf. Sci. 299/300 (1994) 798.
[7] H. Brune, Surf. Sci. Rep. 31 (1998) 121.
[8] M.. Parschau, K. Christmann, Ber. Bunsenges Phys. Chem. 99 (1995) 1376.

[9] M. Parschau, D. Schlatterbeck, K. Christmann, Surf. Sci. 376 (1997) 133.
[10] D. Schlatterbeck, M. Parschau, K. Christmann, Surf. Sci. 418 (1998) 240.
[11] W.R. Tyson, W.A. Miller, Surf. Sci. 62 (1977) 267.
[12] L. Vitos, A.V. Ruban, H.L. Sriver, J. Kollár, Surf. Sci. 411 (1998) 186.
[13] L. Pauling, Die Natur der chemischen Bindung, 2nd edn. Verlag Chemie, Weinheim, 1964.
[14] M. Hansen, Constitution of Binary Alloys, McGraw-Hill, New York, 1958.
[15] F. Holland-Nell, U. Sauerwald, Z. Anorg. Chem. 276 (1954) 155.
[16] J.W. He, D.W. Goodman, J. Phys. Chem. 94 (1990) 496.
[17] J.W. He, D.W. Goodman, J. Phys. Chem. 94 (1990) 1502.
[18] J.A. Rodriguez, R.A. Campbell, D.W. Goodman, Surf. Sci. 244 (1991) 211.
[19] J.A. Rodriguez, R.A. Campbell, D.W. Goodman, J. Vac. Sci. Technol. A 10 (1992) 2540.
[20] K. Christmann, G. Ertl, H. Shimizu, J. Catal. 61 (1980) 397.
[21] J.E. Houston, C.H.F. Peden, D.S. Blair, D.W. Goodman, Surf. Sci. 167 (1986) 427.
[22] G.O. Pötschke, J. Schröder, C. Günther, R.Q. Hwang, R.J. Behm, Surf. Sci. 251 (1991) 592.
[23] G.O. Pötschke, R.J. Behm, Phys. Rev. B 44 (1991) 1442.
[24] C. Günther, S. Günther, E. Kopatzki, R.Q. Hwang, J. Schröder, J. Vrijmoeth, R.J. Behm, Ber. Bunsenges. Phys. Chem. 97 (1993) 522.
[25] C. Günther, J. Vrijmoeth, R.Q. Hwang, R.J. Behm, Phys. Rev. Lett. 74 (1995) 754.
[26] R. Wagner, A. Mohr, K. Christmann, in preparation.
[27] R. Wagner, D. Schlatterbeck, K. Christmann, in preparation.
[28] R. Wagner, Diploma Thesis, Free University of Berlin, 1997.
[29] H. Schlichting, D. Menzel, Surf. Sci. 272 (1992) 27.
[30] P.A. Redhead, Vacuum 12 (1962) 203.
[31] D.A. King, Surf. Sci. 47 (1975) 384.
[32] E. Bauer, F. Bonczek, H. Poppa, G. Todd, Surf. Sci. 53 (1975) 87.
[33] E. Habenschaden, J. Küppers, Surf. Sci. 138 (1983) L147.
[34] S.H. Payne, H.J. Kreuzer, Surf. Sci. 338 (1995) 261.
[35] H. Staude (Ed.), Physikalisch-chemisches Taschenbuch, Akadem. Verlagsges. Geest und Portig KG, Leipzig, 1949., pp. 1183 ff.
[36] A. Mohr, Diploma Thesis, Free University Berlin, 1998 and to be published.
[37] O. Kurtz, Ph.D. Thesis, Free University of Berlin, 1999.
[38] A. Pavlovska, H. Steffen, E. Bauer, Surf. Sci. 195 (1988) 207.
[39] E. Bauer, Ber. Bunsenges. Phys. Chem. 95 (1991) 1315.
[40] H. Röder, R. Schuster, H. Brune, K. Kern, Phys. Rev. Lett. 71 (1993) 2086.
[41] A.K. Schmid, J.C. Hamilton, N.C. Bartelt, R.Q. Hwang, Phys. Rev. Lett. 77 (1996) 2977.
[42] E. Bauer, H. Poppa, G. Todd, F. Bonczek, J. Appl. Phys. 45 (1974) 5164.
[43] J.C. Vickerman, K. Christmann, G. Ertl, P. Heimann, F.J. Himpsel, D.E. Eastman, Surf. Sci. 134 (1983) 367.
[44] M. Paunov, E. Bauer, Appl. Phys. A 44 (1987) 201.
[45] M. Tikhov, M. Stolzenberg, E. Bauer, Phys. Rev. B 36 (1987) 8713.
[46] X. Jiang, D.W. Goodman, Surf. Sci. 255 (1991) 1.